Neuron, Vol. 42, 773–787, June 10, 2004, Copyright ©2004 by Cell Press

Altered Cortical Synaptic Morphology and Impaired Memory Consolidation in Forebrain-Specific Dominant-Negative PAK Transgenic Mice

Mansuo L. Hayashi,[1] Se-Young Choi,[2,4] B.S. Shankaranarayana Rao,[3,6] Hae-Yoon Jung,[1] Hey-Kyoung Lee,[2,5] Dawei Zhang,[2] Sumantra Chattarji,[3] Alfredo Kirkwood,[2] and Susumu Tonegawa[1,*]

[1]The Picower Center for Learning and Memory
Howard Hughes Medical Institute
RIKEN-MIT Neuroscience Research Center
Center for Cancer Research
Department of Biology and
Department of Brain and Cognitive Science
Massachusetts Institute of Technology
Cambridge, Massachusetts 02139

[2]Department of Neuroscience
Mind/Brain Institute
Johns Hopkins University
Baltimore, Maryland 21208

[3]National Center for Biological Sciences
Tata Institute of Fundamental Research
Bangalore 560065
India

Summary

Molecular and cellular mechanisms for memory consolidation in the cortex are poorly known. To study the relationships between synaptic structure and function in the cortex and consolidation of long-term memory, we have generated transgenic mice in which catalytic activity of PAK, a critical regulator of actin remodeling, is inhibited in the postnatal forebrain. Cortical neurons in these mice displayed fewer dendritic spines and an increased proportion of larger synapses compared to wild-type controls. These alterations in basal synaptic morphology correlated with enhanced mean synaptic strength and impaired bidirectional synaptic modifiability (enhanced LTP and reduced LTD) in the cortex. By contrast, spine morphology and synaptic plasticity were normal in the hippocampus of these mice. Importantly, these mice exhibited specific deficits in the consolidation phase of hippocampus-dependent memory. Thus, our results provide evidence for critical relationships between synaptic morphology and bidirectional modifiability of synaptic strength in the cortex and consolidation of long-term memory.

Introduction

The storage or consolidation of declarative memories is thought to involve a reorganization of neural circuits in the cortex as memories are "transferred" from the hippocampus to the cortex (Squire and Alvarez, 1995; Bontempi et al., 1999). However, little is known about the cellular mechanisms underlying cortical memory consolidation, though it has been proposed that one such mechanism is cortical synaptic plasticity (Bear, 1996). This proposal has been supported by a recent study on mice that are heterozygous for a null mutation of α-calcium/calmodulin-dependent protein kinase II (α-CamKII), which exhibited impaired cortical long-term potentiation (LTP) and deficient long-term memory (Frankland et al., 2001).

While the role of LTP in learning and memory has been the focus of many studies (Kandel, 2001; Martin and Morris, 2002; Tonegawa et al., 2003; Nakazawa et al., 2004), a number of theoretical studies have concluded that bidirectional modifiability of synaptic strength, i.e., both LTP and long-term depression (LTD) capacity, is a crucial feature of an effective memory system (Willshaw and Dayan, 1990; Bear and Abraham, 1996; Paulsen and Sejnowski, 2000). This notion has been supported by empirical studies with several lines of genetically engineered mice in which impaired bidirectional modifiability in the hippocampus has been correlated with poor learning capability (Migaud et al., 1998; Huh et al., 2000; Zeng et al., 2001). However, it remains unknown whether bidirectional mofiability in the cortical networks is required for memory consolidation.

A related unresolved issue is whether morphological alterations of cortical synapses critically underlie the consolidation of hippocampus-dependent memory. Evidence has been obtained that indicates that structural changes of dendritic spines accompany LTP and LTD (Luscher et al., 2000; Yuste and Bonhoeffer, 2001): LTP-inducing stimuli have been shown to increase the proportion of larger spines, while LTD-inducing stimuli have been shown to decrease the proportion of larger spines (Toni et al., 1999; Ostroff et al., 2002; Fukazawa et al., 2003; K. Okamoto and Y. Hayashi, personal communication). However, the relationship between cortical spine or synapse morphology and memory consolidation has rarely been explored.

Changes in synaptic morphology are mediated mainly by the remodeling of actin filaments (Matus, 2000). A critical regulator of actin remodeling, which functions downstream of the small GTPases Rac and Cdc42, is p21-activated kinase (PAK), a family of serine-threonine kinases that are composed of at least three members, PAK1, PAK2, and PAK3 (Bokoch, 2003). In neurons, PAK has been shown to regulate synaptic architecture. For example, studies in the fruit fly *Drosophila melanogaster* have shown a requirement for PAK in postsynaptic protein localization (Parnas et al., 2001) as well as in axon guidance (Hing et al., 1999). A recent study in cultured rodent neurons also showed that PAK activity contributes to ephrin B-induced spine formation (Penzes et al., 2003).

The objective of this study is to examine whether an appropriate basal synaptic morphology and bidirec-

*Correspondence: tonegawa@mit.edu
[4]Present address: Department of Physiology, College of Dentistry at Seoul National University, Seoul 110-749 Korea.
[5]Present address: Department of Biology, University of Maryland, College Park, Maryland 20742.
[6]Present address: Department of Neurophysiology, National Institute of Mental Health and Neurosciences, Bangalore 560029 India.

tional synaptic modifiability in the cortex are crucial for the consolidation of hippocampus-dependent long-term memory. Toward this end, we produced transgenic mice in which the expression of a dominant-negative PAK (*dnPAK*) transgene was restricted to the postnatal forebrain. Cortical neurons in these mice had fewer spines and exhibited a shift in the synapse distribution toward synapses of larger size. These alterations in basal synaptic morphology correlated with altered mean synaptic strength and impaired bidirectional modifiability of synaptic strength. Fortunately, spine morphology and synaptic plasticity were normal in the hippocampus of these mice, providing the opportunity to test the relationships between cortical synaptic structure and function and memory consolidation. Indeed, the *dnPAK* mice were specifically impaired in the consolidation phase of spatial memory and context-dependent fear memory. These results provided critical evidence for crucial relationships between synaptic morphology and bidirectional modifiability of synaptic strength in the cortex and consolidation of hippocampus-dependent memory.

Results

Association of Active PAK with the PSD

To investigate the potential role of PAK in synaptic structure and function, we first determined the localization of PAK in the adult brain. As previously shown, all three PAKs are expressed in multiple brain regions, including the cortex and hippocampus (Manser et al., 1995; Allen et al., 1998) (data not shown). In humans, loss-of-function mutations of the *PAK3* gene are associated with nonsyndromic X-linked mental retardation (Allen et al., 1998; Bienvenu et al., 2000). Since activation of PAK catalytic activity requires the liberation of the catalytic domain from the autoinhibitory domain and autophosphorylation at Thr 423 (Lei et al., 2000), we determined the subcellular localization of the active, Thr 423 autophosphorylated form of PAK (p-PAK) by immunostaining with the p-PAK T423 antibody that recognizes phosphorylated forms of all three PAK isoforms. In 2- to 3-week-old cultures of cortical neurons, p-PAK was distributed throughout the cell soma and the dendritic shafts and was largely absent in the axons (Figure 1A, top panel). Double immunostaining showed little colocalization of p-PAK with neurofilament-M (an axon marker; Figure 1A, top panel) or with synaptophysin (a bouton marker; Figure 1A, middle panel) but revealed extensive colocalization with PSD95, a predominant PSD protein, in the dendritic spines (Figure 1A, bottom panel). To determine whether p-PAK was associated with the PSD, a major site of actin remodeling in spines (Colicos et al., 2001), we performed Western blot analyses on three fractions that were prepared from forebrain homogenates. We isolated synaptosomes and separated them into membrane and PSD fractions (Cho et al., 1992) (for details, see the Experimental Procedures). Phosphorylated forms of all three PAKs were present in the PSD fraction as detected by the p-PAK T423 antibody as well as by PAK1 and PAK3 antibodies (Figure 1B). Interestingly, the phosphorylated (but very little unphosphorylated) PAK was detected in the PSD fraction (Figure 1B). Thus, the majority of PAK in the PSD fraction is the phosphorylated PAK, with the phosphorylated PAK3 particularly enriched in this fraction.

To investigate whether PAK activity was regulated by neuronal activity, we performed Western blot analysis to determine the amount of p-PAK following a brief (5 min) treatment with glycine, a protocol that is known to induce LTP in cultured neurons (Lu et al., 2001). In the synaptoneurosome fraction, the level of p-PAK1 increased by $\sim$62% at 10 min and returned to baseline at 30 min following the glycine treatment (Figure 1C). This transient increase in the active PAK level was blocked by the NMDAR antagonist 2-amino-5-phosphonovaleric acid (APV) (Figure 1C), indicating that the p-PAK increase required activation of NMDAR. Since active PAK was associated with the PSD, these results suggest that NMDAR activation elevates PAK activity in the PSD, which could in turn alter spine morphology through PAK's function in actin remodeling.

Generation of Forebrain-Specific *dnPAK* Transgenic Mice

To examine in vivo whether inhibition of PAK catalytic activity results in impairments in spine morphogenesis, synaptic function, and memory, we generated transgenic mice that expressed dnPAK specifically in the postnatal forebrain (Figure 2A). The dnPAK consists of the PAK autoinhibitory domain (AID-PAK), which binds to the catalytic domain of all three PAKs to block their autophosphorylation and consequently the activation of their catalytic activity, leading to inhibition of actin remodeling (Frost et al., 1998; Zhao et al., 1998; Zenke et al., 1999). *dnPAK* was marked with a *myc*-tag sequence fused in-frame to the amino terminus of the AID-PAK sequence. The α-CamKII promoter and SV40 intron/polyadenylation (polyA) sequence were used to drive high expression of the transgene in the postnatal forebrain. Among the nine transgenic founder lines, two (#21 and #110) displayed the highest levels of transgene expression. Northern blot analysis and RNA in situ hybridization showed that *dnPAK* RNA expression was restricted to the forebrain, including the hippocampus (area CA1, CA3, and dentate gyrus) and the cortex (mainly in layers II/III and V/VI) (Figures 2B and 2D). As shown by Western blot analysis, expression of the dnPAK protein product was detected at lower level at postnatal 1 week and increased to higher level at postnatal 4 weeks (Figure 2C). The expression pattern of the dnPAK protein corresponded to that of the *dnPAK* RNA (Figure 2E). Since the expression analyses yielded very similar results for line #21 and #110, we carried out most of the further analyses with line #21.

To determine the extent to which dnPAK inhibits the endogenous PAK catalytic activity in the adult brain, we carried out an in vitro kinase assay (Zenke et al., 1999). When catalytic activity of PAK was stimulated by GTP-γS-Rac in total forebrain homogenates, the activity that was observed in homogenates from transgenic mice was significantly lower compared to wild-type mice ($p < 0.02$; Figure 2F). We also examined the effect of dnPAK on PAK activity by measuring the amount of p-PAK in PSD fractions from wild-type and transgenic mice using Western blot analysis. In both cortex and hippocampus, the level of p-PAK1 was significantly lower ($\sim$59% of

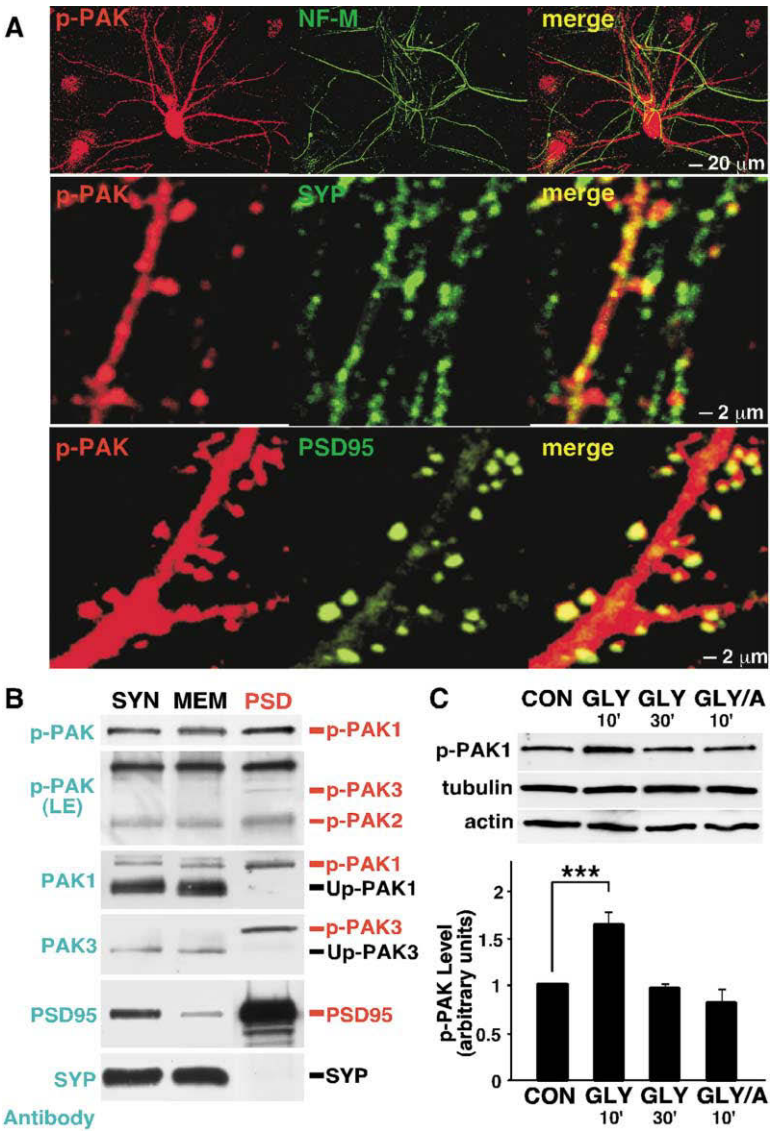

Figure 1. Active PAK Is Associated with the PSD and Elevated by NMDAR Activation

(A) Double staining of cultured cortical neurons for p-PAK T423 (red) and neurofilament-M (NF-M; green in the top panel) or synaptophysin (SYP; green in the middle panel) or PSD95 (green in the bottom panel). p-PAK predominantly localizes in the cell soma, dendrites, and dendritic spines while it is largely excluded from the axons and boutons of mature cortical neurons.

(B) Biochemical fractionation followed by Western blot analysis reveals the presence of active PAK in the PSD fraction. Phosphorylated forms of PAK1, PAK2, and PAK3 (p-PAK1/2/3) were all present in the PSD fraction, while unphosphorylated PAK1/3 (Up-PAK1/3) were nearly absent from the PSD fraction. As detected by the p-PAK antibody, the amount of p-PAK1 was much higher than that of p-PAK2 and p-PAK3. Thus, the film was exposed for a longer time [row p-PAK(LE)] to show the presence of p-PAK2/3 in the PSD fraction. The quality of biochemical fractionation was verified by PSD95 and synaptophysin (SYP) antibodies that detect PSD95 and SYP localizing predominantly in the PSD and membrane fractions, respectively. Lane SYN, synaptosomal preparation; MEM, membrane fraction. Each lane contains 5 μg of total protein.

(C) Western blot analysis reveals that PAK activity is elevated upon NMDAR activation. The gel shows a representative example. The graph depicts the averaged result from five experiments. Tubulin and actin served as internal controls for protein loading. The relative levels of p-PAK1 in each treatment condition are 1 for untreated culture (CON), 1.62 ± 0.13 for culture harvested at 10 min after glycine treatment (GLY 10'), 0.96 ± 0.04 for culture harvested at 30 min after glycine treatment (GLY 30'), and 0.81 ± 0.14 for culture harvested at 10 min after treatment with glycine and APV (GLY/A 10'). ***$p < 0.001$.

the wild-type level in the cortex and ~62% of the wild-type level in the hippocampus) in the 8-week-old transgenic mice compared to wild-type mice ($p < 0.03$; Figure 2G). Because the p-PAK1 level in the hippocampus of wild-type mice was about 2-fold higher than that in the cortex, the residual level of hippocampal p-PAK1 in the transgenic mice was similar to the level of cortical p-PAK1 in the wild-type mice ($p > 0.05$; Figure 2G). At postnatal 3 weeks, the transgene had no effect on the level of p-PAK1 (Figure 2H), presumably reflecting the developmentally delayed activity of the α-CamKII promoter (Figure 2C).

Altered Spine Morphology in the Cortex

The *dnPAK* transgenic mice exhibited normal gross morphology in the forebrain when examined by hematoxylin and eosin staining (data not shown), suggesting that dnPAK does not affect the global anatomy of the forebrain. Since PAK is known to regulate actin remodeling (Bokoch, 2003) and active PAK is localized in dendritic spines (Figure 1), we carried out morphological analysis on the number and structure of spines. In the normal adult brain, the structure of spines is very heterogeneous, and newly formed immature spine-like protrusions are usually smaller and longer than their more mature counterparts (Huber et al., 1998; Toni et al., 2001; Trachtenberg et al., 2002). For the spine analysis, we focused on pyramidal neurons in cortical layer II/III and hippocampal area CA1, two types of cells whose synaptic plasticity has been studied extensively (Diamond et al., 1994; Tsien et al., 1996; Trachtenberg et al., 2000). Golgi staining showed that, in layer II/III of the temporal cortex, the mean density of dendritic spines in the transgenic neurons was lower by ~22% compared to the wild-type neurons ($p < 0.0001$; Figures 3A and 3B). The decreased spine density was observed throughout the proximal to distal segments of the dendrites (Figure 3B) and was not due to nonspecific defects in dendritic arborization, since dendritic length and number of branch points remained unaffected in the transgenic mice (Figure 3D). The transgenic mice also did not differ

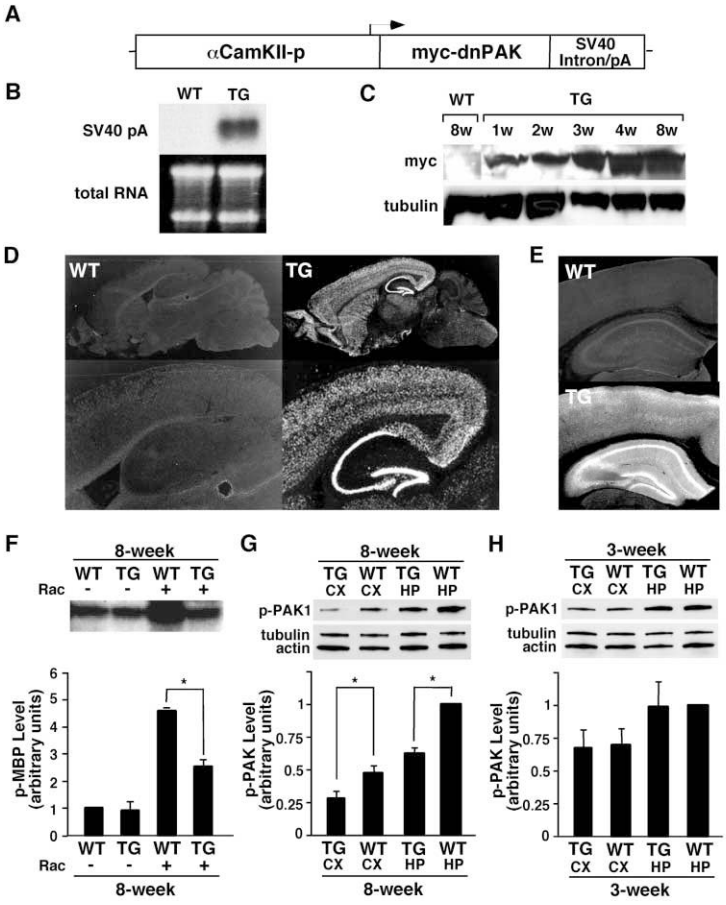

Figure 2. Suppression of PAK Catalytic Activity in the PSD of Forebrain Neurons by Expression of dnPAK

(A) Schematic representation of the *dnPAK* transgene construct.

(B) Northern blot analysis of total RNA from the forebrain of wild-type (WT) and transgenic (TG) mice. The blot was probed with an SV40 pA probe to detect *dnPAK*.

(C) Western blot analysis of forebrain extracts. dnPAK was detected by a *myc* antibody, and tubulin served as an internal control for protein loading.

(D) In situ hybridization of brain sagittal sections with a *myc* probe shows that *dnPAK* is highly expressed in the cortex and hippocampus (images of higher magnification shown at bottom).

(E) Immunostaining with a *myc* antibody detects expression of dnPAK in the cortex and hippocampus.

(F) Catalytic activity of PAK1 in total forebrain homogenates from 8-week-old wild-type and transgenic mice. The activity of immunoprecipitated PAK1 was measured by the amount of phosphorylated myelin basic protein (MBP) in an in vitro kinase assay. The gel shows a representative example. The graph depicts the averaged result from three experiments. GTP-γS-Rac-induced PAK1 activity was significantly inhibited in the transgenic forebrain. *$p < 0.02$.

(G and H) Western blot analysis with the p-PAK T423 antibody in extracts obtained from 8-week-old (G) and 3-week-old (H) mice. The gel shows a representative example. The graph depicts the averaged result from three experiments. (G) In the cortex and hippocampus, phosphorylation of PAK1 was reduced in the PSD fraction of the 8-week-old transgenic mice. The relative levels of p-PAK1 were 0.28 ± 0.05 in the cortex of transgenic mice, 0.47 ± 0.05 in the cortex of wild-type mice, 0.62 ± 0.04 in the hippocampus of transgenic mice, and 1 in the hippocampus of wild-type mice. Tubulin and actin served as internal controls for protein loading. CX, PSD fraction of cortical extracts; HP, PSD fraction of hippocampal extracts. *$p < 0.03$. (H) In the cortex and hippocampus, phosphorylation of PAK1 was not reduced in PSD fraction of the 3-week-old transgenic mice. The relative levels of p-PAK1 were 0.67 ± 0.13 in the cortex of transgenic mice; 0.70 ± 0.12 in the cortex of wild-type mice; 0.99 ± 0.19 in the hippocampus of transgenic mice; and 1 in the hippocampus of wild-type mice.

from wild-type mice in immunostaining intensity and pattern with an axon terminal marker, growth-associated protein 43 (GAP-43) (Goslin et al., 1990) (Supplemental Figure S1 at http://www.neuron.org/cgi/content/full/42/5/773/DC1). This was consistent with the near absence of active PAK in the axons and boutons of mature neurons (Figure 1A). In hippocampal CA1 pyramidal neurons, there was no significant difference in dendritic spine density (Figure 3C) and dendritic length or number of branch points (Figure 3D) between the transgenic and wild-type mice.

To quantitatively compare the structure of individual spines between wild-type and transgenic mice, we first measured spine length (the radial distance from tip of spine head to dendritic shaft) of Golgi-stained pyramidal neurons (Meng et al., 2002). Cortical neurons in the transgenic mice exhibited a significant shift in the overall spine distribution toward spines of shorter length, indicating a lower proportion of longer, filopodia-like spines relative to wild-type neurons (Figure 4A). This is opposite to the increased spine length observed in other forms of mental retardation, including fragile X syndrome (O'Donnell and Warren, 2002). Next, we examined the size of the spine head by conducting electron microscopic analyses of the length of the PSD and the cross-sectional area of the spine head (Figure 4B). As previously shown, these two parameters are representative of the volume of spines and hence can be used to detect changes in spine size (Luo et al., 1996; Toni et al., 2001; Meng et al., 2002). In layer II/III of the temporal cortex, frequency distribution plots revealed a significant shift in the overall distribution toward spines with longer PSD ($p < 0.02$; Kolmogorov-Smirnov test) and larger spine head area ($p < 0.004$; Kolmogorov-Smirnov test) in transgenic neurons relative to wild-type neurons (Figure 4C). Consistently, both mean PSD length ($p < 0.04$) and mean spine head area ($p < 0.02$) of the entire spine population were significantly greater in transgenic than in wild-type neurons in the cortex (Figure 4D). By contrast, the wild-type and transgenic mice did not differ in mean PSD length or in mean spine head area ($p > 0.05$; $n = 3$ mice each) in the hippocampal area CA1.

As visualized in single-section electron micrographs, larger spines often have a discontinuous PSD and are classified as complex or perforated spines, whereas smaller spines always have a continuous PSD and are

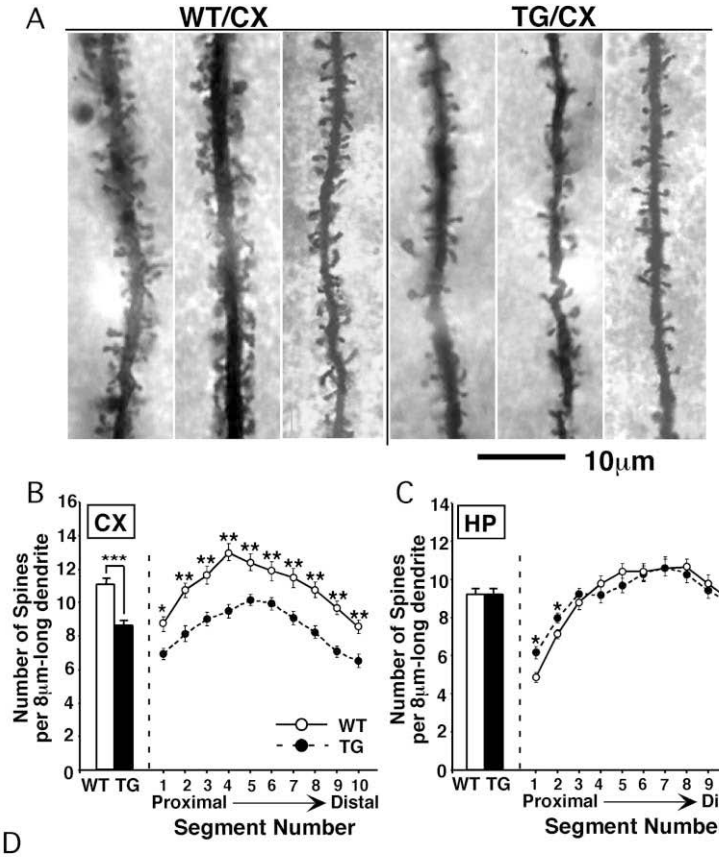

Figure 3. Decreased Spine Density in Cortical Layer II/III Pyramidal Neurons of *dnPAK* Transgenic Mice

(A) Photomicrographs of representative dendritic segments of cortical layer II/III pyramidal neurons from adult wild-type (left) and transgenic (right) mice.

(B) Spine density in primary apical dendrites of layer II/III pyramidal neurons in temporal cortex from wild-type (white) and transgenic (black) mice. (Left) The mean spine density, i.e., the number of spines per 8 μm dendritic segment, was lower in the transgenic (8.45 ± 0.31) than in the wild-type neurons (10.88 ± 0.38; n = 3 mice, 30 neurons each). ***$p < 0.0001$. (Right) Spine density in each 8 μm long dendritic segment is plotted against the consecutive segments, starting with the most proximal (i.e., segment number 1) to the most distal (segment number 10) from the cell soma. Spine density in all segments was significantly lower in transgenic than in wild-type neurons. *$p < 0.05$; **$p < 0.01$.

(C) Spine density in primary apical dendrites of hippocampal CA1 pyramidal neurons. (Left) The mean spine density was indistinguishable between the transgenic (9.16 ± 0.26) and wild-type neurons (9.13 ± 0.25; n = 3 mice, 30 neurons each). (Right) Spine density in most dendritic segments was comparable between transgenic and wild-type neurons. *$p < 0.05$.

(D) Quantitation of the dendritic length and the number of dendritic branch points. There were no significant differences in all of these measures between adult wild-type and transgenic mice in pyramidal neurons in temporal cortical layer II/III and hippocampal area CA1.

D

Type of neuron	Parameter	Dendritic type	WT	TG	*p* values
Temporal cortical layer II/III pyramidal neurons	Dendritic length (μm)	Apical	1242.3±45.6	1277.6±51.5	*p*>0.05
		Basal	1201.0±53.2	1162.3±54.2	*p*>0.05
	Number of branch points	Apical	8.1±0.35	8.1±0.31	*p*>0.05
		Basal	10.3±0.36	10.2±0.36	*p*>0.05
Hippocampal CA1 pyramidal neurons	Dendritic length (μm)	Apical	1790.2±86.3	1764.5±34.2	*p*>0.05
		Basal	1601.5±65.1	1685.7±66.6	*p*>0.05
	Number of branch points	Apical	12.9±0.39	12.8±0.40	*p*>0.05
		Basal	12.1±0.67	11.6±0.41	*p*>0.05

classified as simple spines (Figure 4B) (Calverley and Jones, 1990). In cortical layer II/III, the percentage of perforated spines in the transgenic mice was greater by about 2-fold compared to wild-type controls ($p < 0.03$; Figure 4E). However, the mean size of perforated spines in the transgenic mice (spine head area: 0.21 ± 0.02 μm^2) did not differ from that of wild-type mice (0.21 ± 0.02 μm^2; $p > 0.05$), and the mean size of simple spines was also unaltered in the transgenic mice (0.10 ± 0.01 μm^2 compared to 0.09 ± 0.004 μm^2 in wild-type; $p > 0.05$). This indicates that dnPAK did not promote spine growth per se, rather, dnPAK caused a shift in the spine population from simple to perforated spines, which probably accounts for the increased proportion of larger spines and the enlarged mean spine size in the cortex of transgenic mice.

Collectively, cortical pyramidal neurons in the *dnPAK* transgenic mice had fewer spines and exhibited a shift in the overall spine population toward shorter, larger spines with a perforated PSD compared to wild-type neurons. These results demonstrate a critical role for PAK in dendritic spine morphogenesis and suggest that the level of active PAK influences the extent of spinogenesis.

Altered Presynaptic Structure in the Cortex

In wild-type animals, the PSD matches the presynaptic active zone, and the size of dendritic spines covaries with the number of docked vesicles in the bouton (Harris and Stevens, 1989; Schikorski and Stevens, 1997). To examine whether the structural abnormalities that were observed in the cortical spines of *dnPAK* transgenic mice were accompanied by any presynaptic structural changes, we counted the number of docked vesicles per bouton in wild-type and transgenic mice. Docked vesicles are identified in electron micrographs as the vesicles that abut the plasma membrane of the active zone (Schikorski and Stevens, 1997). In layer II/III of

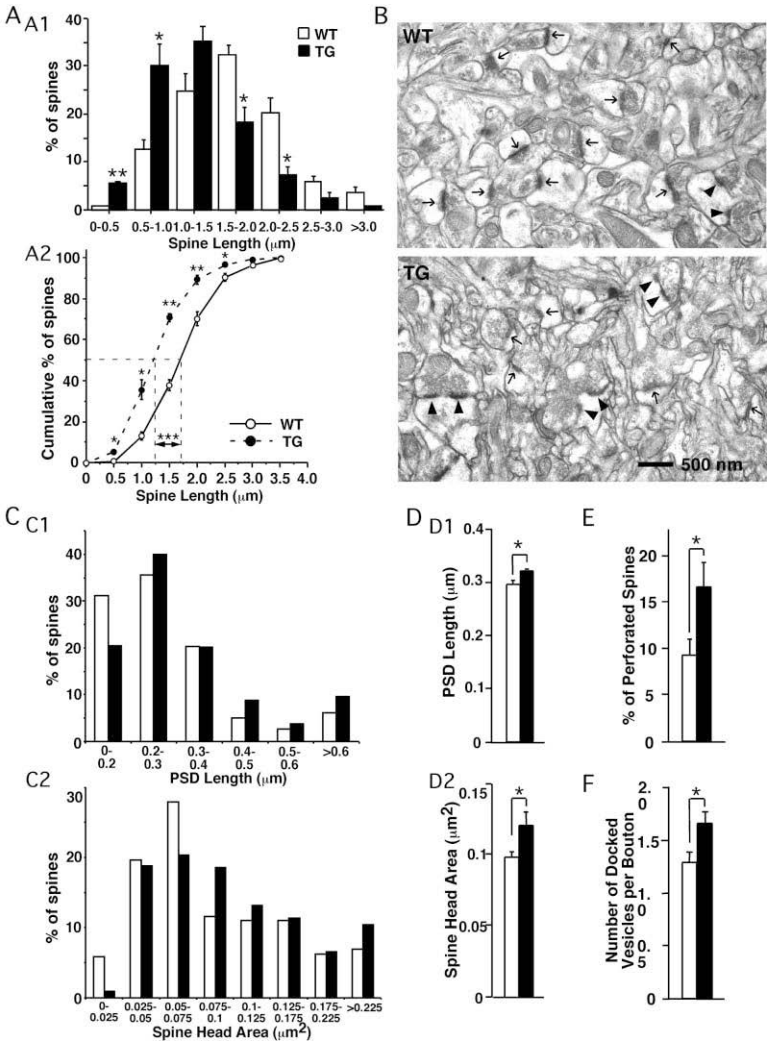

Figure 4. Increased Proportion of Shorter, Larger Spines and Boutons with a Larger Pool of Docked Vesicles in Cortical Layer II/III of the *dnPAK* Transgenic Mice

(A) Frequency distribution plot (A1) and cumulative distribution (A2) of spine length reveal a significant shift in the spine distribution toward spines of shorter length in transgenic neurons (black) relative to wild-type controls (white; n = 3 mice, 30 neurons each). *$p < 0.05$; **$p < 0.01$. The mean spine length was significantly shorter in the transgenic (1.33 ± 0.03 μm) than in the wild-type mice (1.76 ± 0.03 μm). ***$p < 0.001$.

(B) Representative thin-section electron micrographs of layer II/III neuropils in temporal cortex from wild-type and transgenic mice. The PSD is clearly visible as a dark band located right beneath the postsynaptic membrane in the spine head. The spines with arrows indicate simple spines, while the ones with arrowheads indicate perforated spines. The size of perforated spines is on average larger compared to simple spines.

(C) Frequency distribution plots of PSD length (C1) and cross-sectional spine head area (C2) reveal significant shifts in the spine distribution toward spines with longer PSD (Kolmogorov-Smirnov test, $p < 0.02$) and larger spine head area (Kolmogorov-Smirnov test, $p < 0.004$) in transgenic neurons relative to wild-type controls.

(D1) Mean PSD length was significantly longer in the transgenic (0.32 ± 0.002 μm) than in the wild-type mice (0.29 ± 0.01 μm; n = 3 mice, 24 sections each). *$p < 0.04$.

(D2) Mean spine head area was significantly larger in the transgenic (0.12 ± 0.01 μm^2) than in the wild-type mice (0.10 ± 0.004 μm^2). *$p < 0.02$.

(E) The proportion of perforated spines was significantly greater in the transgenic (16.5% ± 2.6%) than in the wild-type mice (9.1% ± 1.8%). *$p < 0.03$.

(F) The mean number of docked vesicles per bouton was significantly greater in the transgenic (1.65 ± 0.11) than in the wild-type mice (1.27 ± 0.10). *$p < 0.02$.

temporal cortex, the transgenic neurons exhibited a significant shift in the overall distribution of boutons toward those with a larger pool of docked vesicles compared to wild-type neurons ($p < 0.001$, Kolmogorov-Smirnov test). Consistently, on average, there was a greater number of docked vesicles per bouton in transgenic than in wild-type mice ($p < 0.02$; Figure 4F). However, the density of docked vesicles (calculated as the number of docked vesicles per unit length of PSD) did not differ between the transgenic (6.82 ± 0.21 per 10 μm) and wild-type mice (6.28 ± 0.28 per 10 μm, $p > 0.05$). Thus, the positive correlation between spine size and docked vesicle number was maintained in the transgenic mice: the increased proportion of larger spines (postsynaptic) in transgenic neurons was accompanied by an increased proportion of boutons with a larger pool of docked vesicles (presynaptic). These results indicate that the proportion of larger synapses was greater in the cortex of transgenic mice relative to wild-type mice.

Enhanced AMPAR- and NMDAR-Mediated Synaptic Transmission in the Cortex

Accumulating evidence has suggested a positive correlation between size of a synapse and the strength of synaptic transmission (Schikorski and Stevens, 1997; Nusser et al., 1998; Mackenzie et al., 1999; Takumi et al., 1999; Matsuzaki et al., 2001; Murthy et al., 2001). To examine whether the increased proportion of larger synapses in the cortex of *dnPAK* transgenic mice correlated with an enhancement in synaptic strength, we first measured miniature excitatory postsynaptic currents (mEPSCs) of cortical neurons. mEPSCs are the spontaneous and randomly occurring synaptic currents that are observed after action potentials have been blocked, and one mEPSC constitutes the response to neurotransmitter released from a single vesicle (Bekkers and Stevens, 1994; Regehr and Stevens, 2001). In layer II/III of temporal cortex, the mean amplitude but not the mean frequency of AMPAR-mediated mEPSCs was greater in

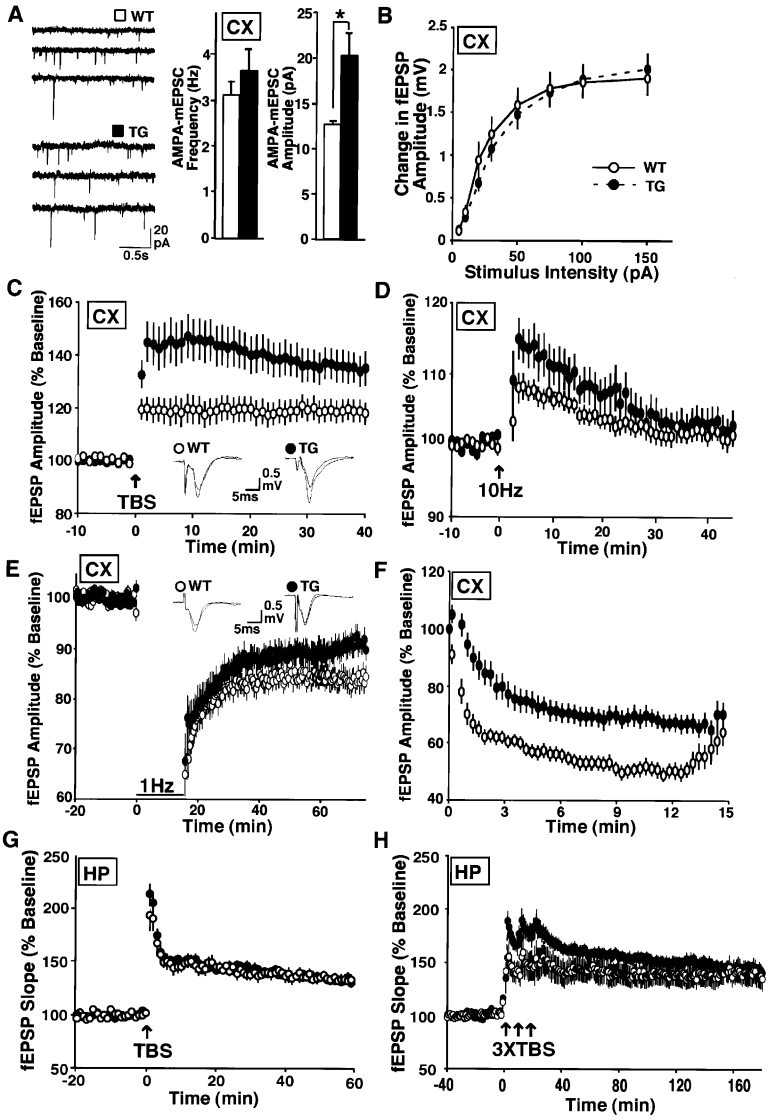

Figure 5. Enhanced Mean Synaptic Strength and Impaired Bidirectional Synaptic Plasticity in the Cortex of *dnPAK* Transgenic Mice

(A) Mean frequency and mean amplitude of AMPAR-mediated mEPSCs in wild-type (white; n = 24 cells, 5 mice) and transgenic neurons (black; n = 18 cells, 4 mice). While the frequency of mEPSCs was comparable between the two genotypes (WT, 3.11 ± 0.30 Hz; TG, 3.61 ± 0.51 Hz; $p > 0.05$), the mean amplitude of mEPSCs was greater in the transgenic (20.24 ± 2.71 pA) than in the wild-type neurons (12.68 ± 0.57 pA). *$p < 0.02$. Example minitraces are shown at the left for each genotype.

(B–H) Extracellular recordings in the temporal cortex layer II/III (B–F) and in the hippocampal area CA1 (G and H) from wild-type (open circle) and transgenic (filled circle) mice.

(B) Input-output curves plotting the changes in fEPSP amplitude and their corresponding presynaptic stimulus intensity. n = 20 slices, 5 mice each.

(C) Cortical LTP induced by TBS was enhanced in transgenic slices (n = 18 slices, 6 mice) relative to wild-type controls (n = 15 slices, 5 mice; $p < 0.04$, repeated-measures ANOVA for 31–40 min). An overlay of representative FP traces taken during baseline and at the last few minutes of recording is shown for each genotype.

(D) Stimulation at 10 Hz produced modestly enhanced potentiation in the transgenic mice (n = 18 slices, 6 mice) relative to wild-type mice (n = 18 slices, 5 mice; $p < 0.007$, interaction of time × genotype of repeated-measures ANOVA for 1–40 min).

(E) Cortical LTD induced by 1 Hz stimulation was significantly impaired in transgenic slices (n = 15 slices, 7 mice) relative to wild-type controls (n = 15 slices, 8 mice; $p < 0.03$, repeated-measures ANOVA for 66–75 min). An overlay of representative FP traces taken during baseline and at the last few minutes of recording is shown for each genotype.

(F) Synaptic depression was significantly impaired throughout the 15 min LFS in transgenic slices relative to wild-type controls ($p < 0.002$, repeated-measures ANOVA for 0–15 min).

(G) CA1 LTP induced by TBS was comparable between transgenic (n = 10 slices, 5 mice) and wild-type slices (n = 8 slices, 5 mice; $p > 0.05$, repeated-measures ANOVA for 51–60 min).

(H) CA1 L-LTP induced by three trains of TBS was comparable between transgenic (n = 11 slices, 6 mice) and wild-type slices (n = 9 slices, 5 mice; $p > 0.05$, repeated-measures ANOVA for 151–180 min). The initial response at 0–40 min was not significantly different between transgenic and wild-type slices ($p > 0.05$, repeated-measures ANOVA).

transgenic neurons than in wild-type neurons ($p < 0.02$; Figure 5A), suggesting an enhancement in mean AMPAR-mediated synaptic transmission in the transgenic mice. Next, we measured the ratio of NMDAR- to AMPAR-mediated synaptic currents and found no statistical difference between the wild-type and transgenic neurons (wt, 0.20 ± 0.01, n = 18 cells, 5 mice; TG, 0.23 ± 0.01, n = 13 cells, 4 mice; $p > 0.05$). Due to the enhanced AMPAR-mediated synaptic transmission, it is likely that mean NMDAR-mediated synaptic transmission was also enhanced in the transgenic mice. Thus, these results suggest that the increased proportion of larger synapses correlated with an enhancement in mean AMPAR- and mean NMDAR-mediated synaptic transmission in the transgenic cortex.

Enhanced LTP and Reduced LTD in the Cortex

To assess whether synaptic plasticity was altered in the transgenic mice, we performed a series of extracellular field recordings from the layer IV to layer II/III synapses in the temporal cortex. The transgenic mice did not differ from wild-type controls in basal synaptic transmission as measured by field potential responses to a range of stimulus intensities (Figure 5B). However, administration of theta-burst stimulation (TBS) at 100 Hz produced LTP with a higher magnitude in transgenic than in wild-type mice ($p < 0.04$, repeated-measures ANOVA for responses at 31–40 min; Figure 5C). Stimulation at 10 Hz produced modestly enhanced potentiation in the transgenic mice relative to wild-type mice ($p < 0.007$, interaction of time × genotype of repeated-measures ANOVA

for responses at 1–40 min; Figure 5D). LTD induced by low-frequency stimulation (LFS, 900 pulses at 1 Hz) was significantly reduced in transgenic slices compared to wild-type controls ($p < 0.03$, repeated-measures ANOVA for responses at 66–75 min; Figure 5E). Interestingly, the decrease in synaptic depression in transgenic slices occurred immediately following the onset of LFS ($p < 0.006$ at 8.5 s) and lasted throughout the 15 min LFS delivery period ($p < 0.002$, repeated-measures ANOVA for responses at 0–15min; Figure 5F). This suggests that the induction phase of LTD was impaired in transgenic mice compared to wild-type mice. In contrast to the abnormal plasticity observed in the cortex, the transgenic mice did not differ from wild-type mice in various stimulation paradigms (basal transmission [data not shown], paired-pulse facilitation [data not shown], TBS-induced LTP [$p > 0.05$, repeated-measures ANOVA for responses at 51–60 min; Figure 5G] and late LTP [L-LTP] induced by three trains of TBS [$p > 0.05$, repeated-measures ANOVA for responses at 151–180 min; Figure 5H]) in the hippocampus. The absence of detectable alteration in synaptic plasticity and spine morphology in the hippocampus of transgenic mice could be explained by the fact that the level of active PAK in the hippocampus of transgenic mice remained similar to that in the cortex of wild-type mice (Figure 2G). Thus, it is possible that PAK inhibition did not reach the critical threshold that is necessary to result in morphological and physiological alterations in the hippocampus. Overall, our results demonstrate a correlation between abnormal synaptic morphology, synaptic strength, and bidirectional modifiability (enhanced LTP and reduced LTD) in the cortical neurons of *dnPAK* transgenic mice.

Normal Acquisition and Impaired Consolidation/Retention of Spatial Memory

To examine whether the structural and electrophysiological defects of the cortical synapses in *dnPAK* transgenic mice lead to deficits in learning and memory, we carried out behavioral analyses. In a battery of tests for general behaviors, including open field, accelerating rotarod, light/dark transition, hot plate, social interaction, and Porsolt's forced swim test (Crowley, 2000), transgenic mice performed similarly to wild-type mice (Supplemental Figure S2 at http://www.neuron.org/cgi/content/full/42/5/773/DC1). This indicates that locomotor activity, pain perception, sensorimotor response, motor coordination, and anxiety level were normal in the transgenic mice.

We then subjected these mice to the hidden-platform version of the Morris water maze, in which the acquisition of spatial memory is known to depend on the hippocampus (Martin and Morris, 2002). The transgenic mice learned as quickly as wild-type mice: the decreases in escape latency (time to reach the platform) and path length (distance traveled to reach the platform) were equivalent between wild-type and transgenic mice (Figure 6A). In the probe trial conducted immediately after the completion of the training session, transgenic mice performed as well as wild-type controls, as indicated by the similar search time in the target quadrant (wt, $43.2\% \pm 3.0\%$, $n = 15$; TG, $44.1\% \pm 4.5\%$, $n = 13$; $p > 0.05$) and the similar number of target platform location crossings (wt, 8.07 ± 1.19; TG, 8.69 ± 1.41; $p > 0.05$; Figure 6B). These results indicate normal learning in *dnPAK* transgenic mice.

Interestingly, the transgenic mice failed to retain their memory compared to wild-type mice, as demonstrated by the comparison of two additional probe trials conducted at 1 and 21 days after the completion of training. At 1 day after training, transgenic mice remembered the platform location equally well as wild-type mice (search time in the target quadrant: wt, $47.4\% \pm 2.3\%$, $n = 34$; TG, $44.5\% \pm 2.2\%$, $n = 34$, $p > 0.05$; number of platform crossings: wt, 8.56 ± 0.77; TG, 7.44 ± 0.66, $p > 0.05$; Figure 6B). By contrast, at 21 days after training, transgenic mice were significantly impaired in the probe trial relative to wild-type mice (search time in the target quadrant: wt, $44.4\% \pm 2.1\%$; TG, $35.5\% \pm 2.5\%$, $p < 0.01$; number of platform crossings: wt, 8.44 ± 0.73; TG, 5.62 ± 0.80, $p < 0.02$; Figure 6B). These results suggest that the acquisition of spatial memory was unaffected while the consolidation/retention of this memory was impaired in the transgenic mice.

Normal Short-Term Contextual Fear Conditioning and Attenuated Consolidation/Retention

To fully study the consequence of cortical structural and physiological alterations on memory consolidation, we subjected the wild-type and transgenic mice to a contextual fear conditioning task, in which the acquisition of contextual fear memory is known to depend on the hippocampus (Tonegawa et al., 2003). The freezing responses were comparable between wild-type and transgenic mice at 40 min (wt, $32.3\% \pm 3.8\%$, $n = 20$; TG, $25.9\% \pm 4.1\%$, $n = 18$, $p > 0.05$; Figure 6C) and 7 hr (wt, $27.1\% \pm 4.0\%$, $n = 20$; TG, $33.9\% \pm 3.9\%$, $n = 17$, $p > 0.05$) after training. However, at 24 hr after training, transgenic mice exhibited a significant reduction in context-dependent freezing relative to wild-type controls (wt, $33.3\% \pm 4.1\%$, $n = 18$; TG, $20.6\% \pm 3.5\%$, $n = 18$, $p < 0.03$; Figure 6C). A similar deficit in long-term contextual fear memory was observed for line #110 (data not shown). In addition, the transgenic mice displayed normal tone-associated memory at 48 hr after training (wt, $32.3\% \pm 4.6\%$, $n = 18$; TG, $31.1\% \pm 3.9\%$, $n = 18$, $p > 0.05$; Figure 6C). These results suggest an impairment in consolidation/retention of contextual fear memory in the transgenic mice, which is consistent with the water maze results.

Discussion

The aim of this study was to investigate the relationship between spine structure and synaptic function in the context of memory capability. To this end, we generated and characterized transgenic mice in which the catalytic activity of PAK, a critical regulator of actin remodeling, was inhibited in postnatal forebrain neurons. In *dnPAK* transgenic mice, cortical neurons had fewer spines and an increased proportion of shorter, larger spines relative to wild-type mice. Cortical synapses of these transgenic mice also displayed a corresponding alteration in the size of boutons. These abnormalities in basal cortical synaptic morphology correlated with enhanced mean synaptic strength and impaired bidirectional modifiabil-

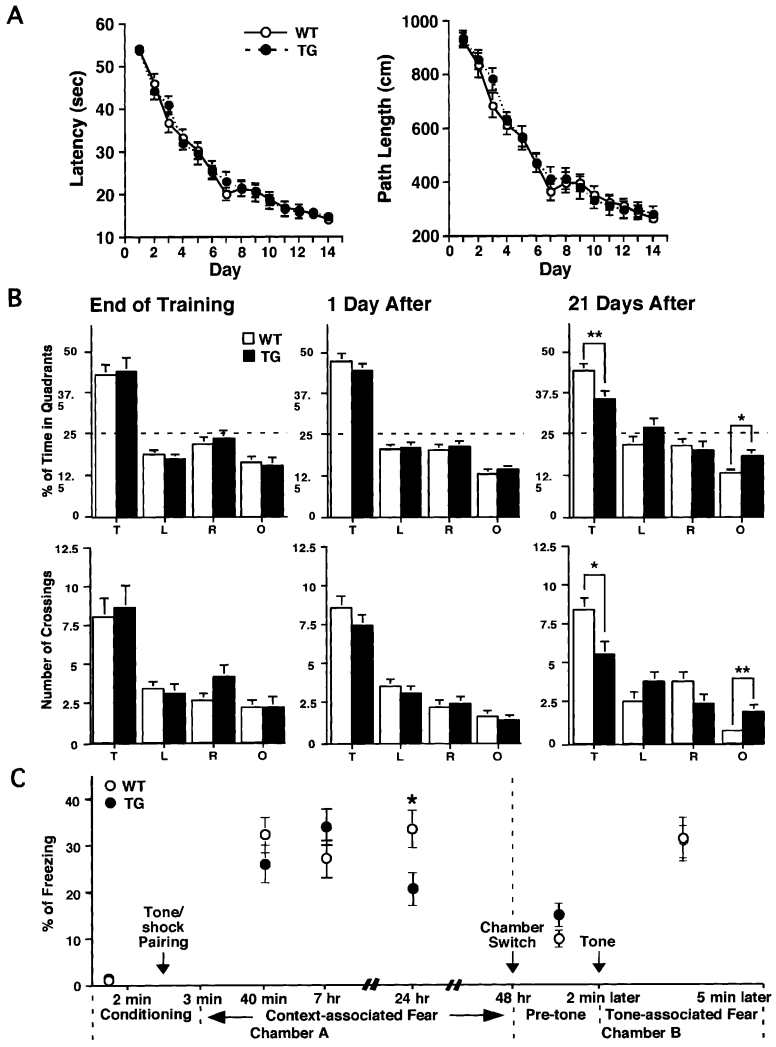

Figure 6. Normal Acquisition and Impaired Consolidation/Retention of Spatial and Contextual Fear Memories in *dnPAK* Transgenic Mice

(A) Normal acquisition of spatial memory in the hidden-platform Morris water maze. The decreases in escape latency (left panel) and path length (right panel) were equivalent between the wild-type (open circle) and transgenic mice (filled circle; n = 34 each, $p > 0.05$, repeated-measures ANOVA).

(B) Results of probe trials given on day 14 (end of training, left), day 15 (1 day after the completion of training, middle), and day 35 (21 days after the completion of training, right). (Upper panel) Mean percent of time spent searching in each quadrant. Dotted lines depict chance level (25%) for random searching. (Lower panel) Mean number of platform crossings. There were significant group differences in both measures on day 35 but not on days 14 and 15. *$p < 0.05$; **$p < 0.01$. T, target quadrant; L, adjacent left quadrant; R, adjacent right quadrant; O, opposite quadrant.

(C) Freezing responses for the wild-type and transgenic mice in fear conditioning. The transgenic mice showed a significantly impaired context-associated fear memory at 24 hr but not at 40 min or 7 hr after conditioning. At 48 hr after conditioning, the transgenic mice exhibited a comparable freezing response to a novel (unconditioned) context ("pre-tone" period) as well as an intact tone-associated fear memory relative to wild-type mice. *$p < 0.03$.

ity (enhanced LTP and reduced LTD). In contrast, spine morphology and synaptic plasticity in the hippocampus were unaltered in *dnPAK* transgenic mice. Notably, *dnPAK* transgenic mice also displayed specific impairments in the consolidation/retention phase of hippocampus-dependent memories. Thus, these results demonstrated a critical role of PAK in cortical spine morphogenesis and suggested critical relationships among basal cortical synaptic structure, bidirectional modifiability of synaptic strength, and long-term memory capability.

Role of PAK in Spinogenesis

Spinogenesis occurs not only during development of the brain but also in adulthood in response to plasticity-inducing stimuli (Moser et al., 1994; Kleim et al., 2002; Knott et al., 2002). A role for PAK in developmental spinogenesis was suggested by a recent in vitro study in which transfection of a dnPAK construct into cultured 10-day-old hippocampal neurons was shown to block ephrin B-induced spine development (Penzes et al., 2003). The lower spine density that was observed in the cortex of *dnPAK* transgenic mice could in part reflect PAK's role in developmental spinogenesis. However, we believe that the contribution of developmental effects should be minimal, since endogenous PAK activity is not detectably inhibited in the transgenic mice through the end of the third postnatal week, by which time developmental spinogenesis is nearly complete in the cortex (Blue and Parnavelas, 1983; Markus and Petit, 1987; Micheva and Beaulieu, 1996). Therefore, it is likely that the lower spine density in transgenic mice indicates a critical role of PAK in activity-induced spinogenesis in the adult brain. Consistent with this role, we found that, in mature neurons, active PAK is associated with the PSD of spines and is elevated upon NMDAR activation.

Through its function in actin remodeling, PAK might mediate de novo spine formation and/or spine duplication: the two proposed modes of activity-dependent spinogenesis (Yuste and Bonhoeffer, 2001). During de novo spine formation (Engert and Bonhoeffer, 1999; Fiala et al., 2002), active PAK could be required for the formation of new protrusions from dendritic shafts (Figure 7A), perhaps by promoting actin polymerization via phosphorylation of LIM kinase and inactivation of cofilin/

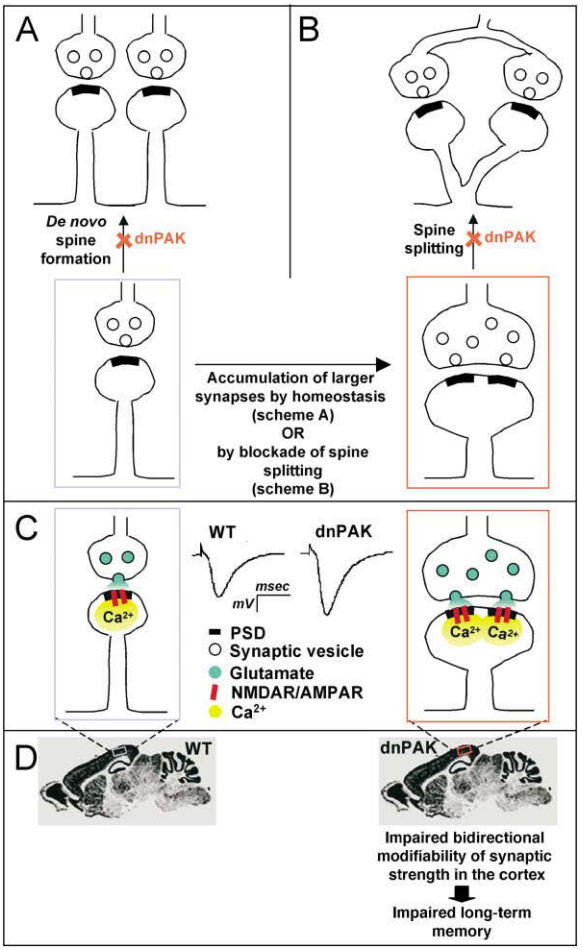

Figure 7. A Model for the Sequence of Events that Lead to the Morphological, Physiological, and Behavioral Alterations in *dnPAK* Transgenic Mice

(A and B) The proposed schemes of activity-dependent spinogenesis and the possible sites of actions by PAK. PAK might mediate de novo spine formation (A) and/or splitting of the enlarged perforated spines in spine duplication (B). In *dnPAK* transgenic mice, due to the homeostatic compensation of reduced de novo formation of simple spines (A) or the failure in splitting larger perforated spines (B), spine density is reduced, and larger synapses with shorter, larger spines with a perforated PSD and correspondingly larger boutons with a larger pool of docked vesicles (indicated in the red frame) accumulate.

(C) Due to the correlation between synapse size and strength of synaptic transmission, the increased proportion of larger synapses in *dnPAK* transgenic mice is associated with enhanced mean synaptic strength (Inset). Presynaptically, these larger synapses would have a larger RRP and possibly a higher release probability of glutamate. Postsynaptically, they exhibit greater AMPAR- and NMDAR-mediated synaptic transmission (likely reflecting more AMPARs and NMDARs), thereby allowing a higher level of NMDAR-mediated Ca^2 influx. For the purpose of simplicity, AMPARs and NMDARs are indicated by the same symbols.

(D) The increased proportion of larger, stronger synapses in cortical neurons of *dnPAK* transgenic mice (indicated by the red frame) correlates with impaired bidirectional modifiability of synaptic strength in the cortex, which might underlie impaired long-term memory.

actin-depolymerizing factor (Edwards et al., 1999). In this case, the increased proportion of larger perforated spines (which usually represent stronger synapses, see below) that is observed in *dnPAK* transgenic mice could be explained as a consequence of homeostatic compensation (Turrigiano and Nelson, 2000) for reduced spine number, in order to maintain the overall output of individual neurons (Figure 7A). Alternatively, during spine duplication in which preexisting spines enlarge, undergo PSD perforation, and split to form new *simple* spines (Toni et al., 1999, 2001), active PAK could be required for the splitting of the enlarged perforated spines (Figure 7B), possibly by disassembling actin-myosin filaments that associate with the spine plasma membrane (Morales and Fifkova, 1989) via phosphorylation and inactivation of myosin light chain kinase (Sanders et al., 1999). In this case, PAK inhibition would directly lead to a greater proportion of larger perforated spines in the transgenic mice (Figure 7B).

Association between Synapse Size and Strength of Synaptic Transmission

In a synapse, spine size has been shown to correlate with bouton size and the number of docked vesicles in the bouton (Harris and Stevens, 1989; Schikorski and Stevens, 1997). Consistent with these observations, we found that the increased proportion of larger spines in transgenic cortical neurons correlated with an increased proportion of boutons with a larger pool of docked vesicles, while the density of docked vesicles did not differ between transgenic and wild-type neurons. Since the docked vesicle pool coincides with the readily-releasable pool (RRP) that determines the probability of neurotransmitter release (Murthy et al., 2001), our results suggested a larger RRP and possibly a greater release probability per synapse in the transgenic neurons (Figure 7C). A greater release probability per synapse together with a lower synapse number (due to the lower spine density) could explain the unaltered frequency of AMPAR-mediated mEPSC that was observed in the transgenic neurons. Since endogenous active PAK is nearly absent in the axons and boutons of mature neurons, the observed presynaptic alteration is likely a secondary effect of the postsynaptic alteration, perhaps occurring through communication between pre- and postsynaptic terminals via various molecules, including cell adhesion molecules and secreted proteins (Scheiffele, 2003).

Spine size has also been shown to correlate with the strength of synaptic transmission, as larger spines have more AMPARs and NMDARs than smaller spines (Nusser et al., 1998; Mackenzie et al., 1999; Takumi et al., 1999; Matsuzaki et al., 2001). We did not directly examine the number of AMPARs and NMDARs; however, we observed a greater mean amplitude of AMPAR-mediated mEPSCs as well as an unaltered ratio of NMDAR- to AMPAR-mediated synaptic currents in transgenic cortical neurons relative to wild-type controls. These observations suggested enhanced mean AMPAR- and NMDAR-mediated synaptic transmission in the transgenic neurons, thus providing evidence for an association between spine size and strength of synaptic transmission (Figure 7C). Taken together, our findings from

pre- and postsynaptic terminals in cortical synapses of *dnPAK* transgenic mice indicated that the shift in spine distribution toward spines of larger size was associated with a shift in the corresponding synapse distribution toward synapses of larger size and stronger transmission.

Cortical Bidirectional Modifiability of Synaptic Strength and Long-Term Memory Storage

Accumulating evidence has suggested that bidirectional modifiability of synaptic strength is critical for a neural network to function as an effective memory system (Willshaw and Dayan, 1990; Migaud et al., 1998; Huh et al., 2000; Paulsen and Sejnowski, 2000; Zeng et al., 2001). Consistent with this notion, *dnPAK* transgenic mice, which exhibited behavioral deficits in the consolidation/retention of spatial and contextual fear memories, displayed impaired bidirectional modifiability, namely, enhanced LTP and reduced LTD, in the temporal cortex (Figure 7D). It is possible and even likely that the alterations in synaptic morphology and plasticity are not restricted to the temporal cortex and occur in other cortical areas. However, the behavioral deficits were highly specific to the consolidation/retention and not observed in the acquisition of these hippocampus-dependent memories, strongly suggesting that sufficiently normal wiring and computational functions are maintained in the forebrain of the transgenic mice. Indeed, associated with their normal acquisition of these hippocampus-dependent memories (Figure 6), we found normal hippocampal synaptic plasticity (LTP and L-LTP) in *dnPAK* transgenic mice (Figures 5G and 5H). A similar dissociation between hippocampal and cortical plasticity was previously observed in mice heterozygous for a null mutation of α-CamKII (α-*CamKII* $^{/}$) (Frankland et al., 2001). These mice, which had impaired cortical LTP and normal hippocampal LTP and L-LTP, exhibited deficits in memory consolidation but not memory acquisition. Our study has confirmed this finding by identifying correlatory impairments in bidirectional modifiability of synaptic strength specifically in the cortex and memory consolidation and further shown that abnormalities of basal synaptic morphology also correlate.

In the literature, there have been very few studies about the temporal onset of cortical function in the consolidation of hippocampus-dependent memory—even fewer when it comes to the comparison between Morris water maze and contextual fear conditioning. The only relevant study in the literature is the one by Frankland et al. (2001), in which the α-*CamKII* $^{/}$ mutants displayed impairments on day 3 posttraining in contextual fear conditioning and on day 10 in the water maze task. These data are similar to ours in that *dnPAK* transgenic mice show impairments on day 1 in contextual fear conditioning and on day 21 in the water maze. The onset timing of cortical consolidation would vary depending on a variety of factors, including the type of memory tasks and the training protocols. In addition, the type and extent of the cortical gene manipulation would certainly affect the timing of detectable deficit. Future studies employing genetic and pharmacological perturbations in the cortex will help to determine the onset timing of cortical consolidation in specific types of memory tasks.

Underlying Mechanism of Impaired Bidirectional Modifiability

How does the inhibition of PAK activity lead to the impaired bidirectional modifiability in *dnPAK* transgenic mice? In principle, the impaired bidirectional modifiability could reflect either a direct effect of PAK inhibition or an indirect outcome of PAK inhibition, perhaps through alteration in basal synaptic structure. Interestingly, the effects of PAK inhibition on bidirectional plasticity are already apparent in the induction phase while, as previously shown, it is not the induction phase but the maintenance phase of plasticity that requires actin remodeling (Krucker et al., 2000; Fukazawa et al., 2003), which likely involves PAK activity. Thus, it is likely that inhibition of PAK activity in the transgenic mice does not directly account for the altered induction of plasticity. Rather, we believe that the altered induction of bidirectional plasticity reflects the altered basal distribution of synapse size.

Previous studies have identified a few key variables that determine the sign of bidirectional modifiability, i.e., whether a synapse undergoes LTP or LTD following stimulation. It is thought that a synapse is more likely to undergo potentiation and less likely to undergo depression if it exhibits slower vesicle depletion presynaptically and/or a higher level of NMDAR-mediated Ca^2 influx postsynaptically (Malenka and Nicoll, 1993; Gottschalk et al., 1998; Huber et al., 1998; Lisman, 2001). The larger cortical synapses in *dnPAK* transgenic mice could fulfill both of these criteria. Presynaptically, these larger boutons would exhibit slower vesicle depletion because they have a larger pool of docked vesicles than smaller boutons (Zucker, 1989; Dobrunz and Stevens, 1997; Murthy et al., 2001). Postsynaptically, these larger spines would allow more NMDAR-mediated Ca^2 influx because they have more NMDARs as well as more AMPARs that can produce greater depolarization, leading to enhanced NMDAR activation relative to smaller spines (Mackenzie et al., 1999; Matsuzaki et al., 2001). Thus, the increased proportion of larger synapses in the transgenic mice would result in an increased proportion of potentiated synapses following TBS, leading to enhanced LTP, but a decreased proportion of depressed synapses following LFS, leading to reduced LTD. Hence, by modulating the induction of plasticity, the shift in basal synapse distribution toward larger synapses would impair bidirectional modifiability of the network favoring LTP over LTD. Consistent with this possibility, an increased proportion of larger spines has recently been observed in the visual cortex of dark-reared rats, which exhibits enhanced LTP and reduced LTD (Kirkwood et al., 1996) (W. Wallace and M.F. Bear, personal communication). Strikingly, in these rats, exposure to light reverses the altered basal distribution of spine size as well as the impaired bidirectional modifiability.

Taken together, the correlatory observations of altered distribution of synapse size and impaired bidirectional modifiability of synaptic strength in the cortex and deficient memory consolidation in *dnPAK* transgenic mice lead us to propose that the basal distribution of synapse size in the cortex must be within a range that is appropriate for bidirectional modifiability in order for a population of neurons to function as an effective memory network. Thus, in addition to structural plasticity of

individual synapses, memory consolidation would depend on the basal synaptic structure in a population of synapses in the cortex. Future studies employing genetic or pharmacological perturbations will help to further understand how basal synaptic structure affects bidirectional modifiability and memory capability. Hopefully, such studies will provide mechanistic insight into the causes of cognitive dysfunction in mental retardation, since many of the genes that are implicated in mental retardation, including *PAK3*, are involved in the regulation of synaptic structure (Chelly and Mandel, 2001).

Experimental Procedures

Generation of Transgenic Mice

The *dnPAK* transgene construct contained the 8.5 kb α-CamKII promoter, *myc*-tagged AID-PAK, and SV40 intron/polyA (from pMSG [Pharmacia]). The cDNA for AID-PAK, encoding amino acids (aa) 78–146 of PAK3 (corresponding to aa 83–149 of PAK1) (Zhao et al., 1998), was amplified by polymerase chain reaction from mouse cDNA and cloned into the pCMV-6*myc* vector to generate an in-frame fusion between the N terminus of AID-PAK and the C terminus of the *myc* tag. The *myc*-tagged AID-PAK fragment was then cloned between the α-CamKII promoter and SV40 intron/polyA to generate pMLH101. The 10 kb SalI fragment of pMLH101 containing the *dnPAK* transgene was purified and microinjected into C57BL6 zygotes to generate transgenic mice. All wild-type and transgenic mice used in this study are of the C57BL6 genetic background.

Northern Blot Analysis and In Situ Hybridization

Total RNA was isolated from mouse forebrains, and RNA blots were hybridized to ^{32}P-labeled DNA probes containing SV40 intron/polyA to detect expression of *dnPAK*. For in situ hybridization, frozen mouse brains were sectioned (14 μm) with a cryostat (Leica), fixed, and hybridized with ^{33}P-labeled RNA probes.

Western Blot Analysis, PSD Fractionation, and Kinase Assay

Mouse forebrains were homogenized in RIPA buffer (50 mM Tris-HCl pH 7.5, 150 mM NaCl, 1% NP-40, 0.5% sodium deoxycholate, 1 mM DTT, and proteinase inhibitors). Biochemical fractionation of forebrain extracts was carried out by sucrose gradient centrifugation (Cho et al., 1992). The PSD and membrane fractions were the Triton-insoluble and -soluble fractions from synaptosome, respectively. These fractions were subjected to Western blot analysis using the p-PAK1 Thr 423 antibody (Cell Signaling) that recognizes the phosphorylated forms of all three PAKs: PAK1 phosphorylated at Thr 423, PAK2 phosphorylated at Thr 402, and PAK3 phosphorylated at Thr 421. Other antibodies used include the myc (RDI), tubulin (BabCo), actin (Santa Cruz), PAK1 (Santa Cruz), PAK3 (Upstate), PSD95 (Upstate), and synaptophysin (Chemicon) antibodies. To determine the level of p-PAK, the synaptoneurosome fraction was isolated and then incubated with 0.5% Triton for 15 min on ice to obtain the PSD fraction (Johnson et al., 1997). In Western blot analysis, the level of p-PAK1 in the hippocampus of wild-type mice was always defined as 100%. The relative level of p-PAK was quantified from the scanned films using the OpenLab Software Program (Improvision). To determine the catalytic activity of PAK using an in vitro kinase assay (Zenke et al., 1999), the phosphorylated products were resolved by SDS-PAGE and quantified with a Fujix Bioimaging Analyzer. To determine the regulation of PAK activity by neuronal activity, 2- to 3-week-old cultures were treated with glycine (100 μM), with or without APV, for 5 min (Lu et al., 2001). At different times after treatment, synaptoneurosome fractions were obtained from culture extracts and subjected to Western blot analysis.

Immunostaining

Primary cortical neurons prepared from rat pups at postnatal day 1 (Renger et al., 2001) and cultured for 2–3 weeks were fixed with 4% paraformaldehyde (PFA) and stained with the p-PAK T423 and NF-M (Zymed) or synaptophysin or PSD95 antibodies. For immunostaining of brain slices, 4%-PFA-perfused brains were sectioned (50 μm) and stained with the *myc* antibody. To visualize axonal terminals, paraffin-embedded sections (8 μm) were stained with the GAP43 antibody (Chemicon) and counterstained with NeuroTrace Nissl stains (Molecular Probes).

Golgi Analysis

From 2-month-old male littermates, 120 μm thick serial sections were obtained following the Golgi-Cox technique (Ramon-Moliner, 1970). Slides containing these sections were coded before quantitative analysis, and the code was broken only after the analysis was completed. Camera lucida tracings (500×) were obtained (Leitz Orthoplan) and then scanned at 1200 dpi for subsequent computerized image analysis with custom-designed macros embedded in Object Image software (Vyas et al., 2002). Spine density was quantified in the same population of neurons that were used for dendritic morphometry. On each primary apical dendritic branch, ten consecutive 8 μm long dendritic segments were analyzed to quantify spine density. To ensure sampling consistency among Golgi analysis, electron microscopy, and electrophysiological experiments, analyses in the hippocampal area CA1 were all carried out in slices or sections corresponding to Figures 45 to 48 of the mouse brain atlas (Franklin and Paxinos, 1997), and analyses in the temporal cortex were all carried out in slices or sections corresponding to Figures 62 to 67.

Electron Microscopy

Two-month-old male littermates were anesthetized and perfused as previously described (Fiala et al., 1998). Blocks of hippocampus and of temporal cortex were embedded, from which 1 μm thick sections were cut and stained with 1% toluidine blue to guide the further trimming to isolate regions of interest, i.e., CA1 stratum radiatum (~150 μm from the CA1 cell body layer) or layer II/III of temporal cortex. Ultrathin sections (90 nm) were then cut and stained with uracyl acetate and lead citrate. Randomly selected neuropil areas were photographed at a 10,000× magnification with a JEOL 1200EX electron microscope. Image negatives were scanned at 1200 dpi and analyzed by OpenLab Program (Improvision). Excitatory synapses bearing spines were defined by the presence of a clear PSD facing at least three presynaptic vesicles (Luo et al., 1996; Meng et al., 2002). Micrographs covering 500–1000 μm^2 neuropil regions from either hippocampus or cortex of each mouse were analyzed and used for quantitation. PSD length, cross-sectional area of spine head, percentage of perforated spines, and number of presynaptic docked vesicles were quantified from the same population of synapses. The measurements were all performed by an experimenter blind to the genotype.

Electrophysiology

From 2- to 3-month-old male littermates, transverse hippocampal slices and coronal brain slices containing temporal cortex were prepared and left to recover for at least 1 hr before recording in oxygenated (95% O_2 and 5% CO_2) warm (30 C except at 25 C for hippocampal LTP experiment) artificial cerebrospinal fluid (ACSF) containing 124 mM NaCl, 5 mM KCl, 1.25 mM NaH_2PO_4, 1 mM $MgCl_2$, 2 mM $CaCl_2$, 26 mM $NaHCO_3$, and 10 mM dextrose. CA1 field potentials (FP) evoked by Schaffer collateral stimulation and FP in layer II/III evoked by layer IV stimulation were measured as previously described (Kirkwood et al., 1996; Frankland et al., 2001). Responses were quantified either as the initial slope of FP in CA1 or as the amplitude of FP in cortex. Cortical LTP was induced by TBS, which consisted of eight brief bursts (each with four pulses at 100 Hz) of stimuli delivered every 200 ms. Stimulation (10 Hz) consisted of three trains (each with 32 pulses at 10 Hz) delivered at 2 s intervals. LTD stimulation consisted of 900 pulses of stimuli at 1 Hz for 15 min. Hippocampal LTP was induced by TBS consisting of ten bursts, and L-LTP was induced by three trains of TBS (each with eight bursts) at 10 min intervals. For measurement of AMPAR-mediated mEPSC (Lee et al., 2003), 1 μM tetrodotoxin, 100 μM APV, and 10 μM bicuculline were added in bath ACSF. The cells were held at 80 mV, and recordings were done at 30 C. Continuous 30–60 ms traces were collected at 8 s intervals and filtered at 2 KHz. Cells with series resistance 13 m were discarded. The measurement

of NMDAR-EPSC/AMPAR-EPSC ratio was done in ACSF containing 2 mM Mg^{2} , 10 μM bicuculline, and 50 μM glycine as described (Myme et al., 2003). NMDAR-dependent and AMPAR-dependent responses were discriminated based on their distinct kinetics and voltage dependence. Thus, as an index of the NMDAR-mediated response, we used the value of the currents recorded at 40 mV and measured 100 ms after the response onset. The AMPAR-mediated response was taken from the peak amplitude response recorded at 80 mV.

Behavioral Tests

Animals used were all male littermates at 2–4 months of age. Open field, accelerating rotarod, light/dark transition, hot plate, social interaction, and Porsolt's forced swim tests were all carried out as previously described (Crowley, 2000). The hidden platform Morris water maze was carried out as previously described (Zeng et al., 2001). Mice were subjected to water maze training at four trials per day with intertrial intervals of 3 min. Each training trial ended either when the mice reached the platform or after 60 s elapsed. Probe trials, i.e., 60 s swimming sessions in the absence of platform, were conducted at 1 hr, 1 day, or 21 days after the last training session. Mice that were tested for several probe trials were always trained for an extra four-trial session after the previous probe trial to prevent memory extinction. The swimming traces were digitized and analyzed by Image WM program (O'Hara & Co). Fear conditioning was carried out as previously described (Zeng et al., 2001). On day 1, mice were placed in the training chamber (Coulbourn Instruments) (chamber A) for 2 min before the onset of a 30 s white noise tone that coterminated with a 2 s shock (0.7 mA intensity), after which mice remained for another 30 s. To test contextual memory, at 40 min, 7 hr, or 24 hr after training, mice were placed back into chamber A for 3 min. Video images were digitized, and the percentage of freezing time was analyzed by Image FZ program (O'Hara & Co). Freezing was defined as the absence of all but respiratory movement for a consecutive 2 s period. To test tone-associated memory, on day 3, mice were placed into a new chamber (chamber B) with a different shape and smell from chamber A for 2 min before the onset of a 3 min tone. To avoid the confounding effects of extinction, separate groups of mice were tested at each retention delay.

Animal Handling, Experimental Design, and Data Analysis

The generation and maintenance of mice and all experimental procedures were performed in compliance with National Institute of Health guidelines. All experiments were conducted in a blind fashion. Statistical analyses were carried out using Statview software (SAS). Unless specified otherwise, data were analyzed with Student's t test; p values greater than 0.05 were regarded as not significant. Values are presented as mean ± SEM.

Acknowledgments

We are grateful of Xiaoning Zhou, Wenjiang Yu, Frank Bushard, and Jayson Derwin for excellent technical assistance. We thank Drs. David Gerber, Thomas McHugh, Matthew Anderson, Audrey Chang, Yasunori Hayashi, Guo-song Liu, Morgan Sheng, and Mark Bear for critical discussions; many members of the Tonegawa lab for helpful advice; Dr. Tsuyoshi Miyakawa for advice on behavioral experiments; Marcia Feinberg, Maria Ericsson, Elizabeth Benecchi, and Dr. Kristen Harris for help on electron microscopy. This study was supported by NIH, HHMI, and RIKEN (S.T.) and NIH (A.K.).

Received: February 11, 2004
Revised: April 23, 2004
Accepted: May 6, 2004
Published: June 9, 2004

References

Allen, K.M., Gleeson, J.G., Bagrodia, S., Partington, M.W., MacMillan, J.C., Cerione, R.A., Mulley, J.C., and Walsh, C.A. (1998). PAK3 mutation in nonsyndromic X-linked mental retardation. Nat. Genet. *20*, 25–30.

Bear, M.F. (1996). A synaptic basis for memory storage in the cerebral cortex. Proc. Natl. Acad. Sci. USA *93*, 13453–13459.

Bear, M.F., and Abraham, W.C. (1996). Long-term depression in hippocampus. Annu. Rev. Neurosci. *19*, 437–462.

Bekkers, J.M., and Stevens, C.F. (1994). Molecular and Cellular Mechanisms of Neurotransmitter Release (New York: Raven Press).

Bienvenu, T., des Portes, V., McDonell, N., Carrie, A., Zemni, R., Couvert, P., Ropers, H.H., Moraine, C., van Bokhoven, H., Fryns, J.P., et al. (2000). Missense mutation in PAK3, R67C, causes X-linked nonspecific mental retardation. Am. J. Med. Genet. *93*, 294–298.

Blue, M.E., and Parnavelas, J.G. (1983). The formation and maturation of synapses in the visual cortex of the rat. II. Quantitative analysis. J. Neurocytol. *12*, 697–712.

Bokoch, G.M. (2003). Biology of the p21-activated kinases. Annu. Rev. Biochem. *72*, 743–781.

Bontempi, B., Laurent-Demir, C., Destrade, C., and Jaffard, R. (1999). Time-dependent reorganization of brain circuitry underlying long-term memory storage. Nature *400*, 671–675.

Calverley, R.K., and Jones, D.G. (1990). Contributions of dendritic spines and perforated synapses to synaptic plasticity. Brain Res. Brain Res. Rev. *15*, 215–249.

Chelly, J., and Mandel, J.L. (2001). Monogenic causes of X-linked mental retardation. Nat. Rev. Genet. *2*, 669–680.

Cho, K.O., Hunt, C.A., and Kennedy, M.B. (1992). The rat brain postsynaptic density fraction contains a homolog of the Drosophila discs-large tumor suppressor protein. Neuron *9*, 929–942.

Colicos, M.A., Collins, B.E., Sailor, M.J., and Goda, Y. (2001). Remodeling of synaptic actin induced by photoconductive stimulation. Cell *107*, 605–616.

Crowley, J.N. (2000). What's Wrong with My Mouse? Behavioral Phenotyping of Transgenic and Knockout Mice (New York: Wiley).

Diamond, M.E., Huang, W., and Ebner, F.F. (1994). Laminar comparison of somatosensory cortical plasticity. Science *265*, 1885–1888.

Dobrunz, L.E., and Stevens, C.F. (1997). Heterogeneity of release probability, facilitation, and depletion at central synapses. Neuron *18*, 995–1008.

Edwards, D.C., Sanders, L.C., Bokoch, G.M., and Gill, G.N. (1999). Activation of LIM-kinase by Pak1 couples Rac/Cdc42 GTPase signalling to actin cytoskeletal dynamics. Nat. Cell Biol. *1*, 253–259.

Engert, F., and Bonhoeffer, T. (1999). Dendritic spine changes associated with hippocampal long-term synaptic plasticity. Nature *399*, 66–70.

Fiala, J.C., Feinberg, M., Popov, V., and Harris, K.M. (1998). Synaptogenesis via dendritic filopodia in developing hippocampal area CA1. J. Neurosci. *18*, 8900–8911.

Fiala, J.C., Allwardt, B., and Harris, K.M. (2002). Dendritic spines do not split during hippocampal LTP or maturation. Nat. Neurosci. *5*, 297–298.

Franklin, K.B.J., and Paxinos, G. (1997). The Mouse Brain in Stereotaxic Coordinates (San Diego: Academic).

Frankland, P.W., O'Brien, C., Ohno, M., Kirkwood, A., and Silva, A.J. (2001). Alpha-CaMKII-dependent plasticity in the cortex is required for permanent memory. Nature *411*, 309–313.

Frost, J.A., Khokhlatchev, A., Stippec, S., White, M.A., and Cobb, M.H. (1998). Differential effects of PAK1-activating mutations reveal activity-dependent and -independent effects on cytoskeletal regulation. J. Biol. Chem. *273*, 28191–28198.

Fukazawa, Y., Saitoh, Y., Ozawa, F., Ohta, Y., Mizuno, K., and Inokuchi, K. (2003). Hippocampal LTP is accompanied by enhanced F-actin content within the dendritic spine that is essential for late LTP maintenance in vivo. Neuron *38*, 447–460.

Goslin, K., Schreyer, D.J., Skene, J.H., and Banker, G. (1990). Changes in the distribution of GAP-43 during the development of neuronal polarity. J. Neurosci. *10*, 588–602.

Gottschalk, W., Pozzo-Miller, L.D., Figurov, A., and Lu, B. (1998). Presynaptic modulation of synaptic transmission and plasticity by brain-derived neurotrophic factor in the developing hippocampus. J. Neurosci. *18*, 6830–6839.

Harris, K.M., and Stevens, J.K. (1989). Dendritic spines of CA 1 pyramidal cells in the rat hippocampus: serial electron microscopy with reference to their biophysical characteristics. J. Neurosci. *9*, 2982–2997.

Hing, H., Xiao, J., Harden, N., Lim, L., and Zipursky, S.L. (1999). Pak functions downstream of Dock to regulate photoreceptor axon guidance in *Drosophila*. Cell *97*, 853–863.

Huber, K.M., Sawtell, N.B., and Bear, M.F. (1998). Brain-derived neurotrophic factor alters the synaptic modification threshold in visual cortex. Neuropharmacology *37*, 571–579.

Huh, G.S., Boulanger, L.M., Du, H., Riquelme, P.A., Brotz, T.M., and Shatz, C.J. (2000). Functional requirement for class I MHC in CNS development and plasticity. Science *290*, 2155–2159.

Johnson, M.W., Chotiner, J.K., and Watson, J.B. (1997). Isolation and characterization of synaptoneurosomes from single rat hippocampal slices. J. Neurosci. Methods *77*, 151–156.

Kandel, E.R. (2001). The molecular biology of memory storage: a dialogue between genes and synapses. Science *294*, 1030–1038.

Kirkwood, A., Rioult, M.C., and Bear, M.F. (1996). Experience-dependent modification of synaptic plasticity in visual cortex. Nature *381*, 526–528.

Kleim, J.A., Barbay, S., Cooper, N.R., Hogg, T.M., Reidel, C.N., Remple, M.S., and Nudo, R.J. (2002). Motor learning-dependent synaptogenesis is localized to functionally reorganized motor cortex. Neurobiol. Learn. Mem. *77*, 63–77.

Knott, G.W., Quairiaux, C., Genoud, C., and Welker, E. (2002). Formation of dendritic spines with GABAergic synapses induced by whisker stimulation in adult mice. Neuron *34*, 265–273.

Krucker, T., Siggins, G.R., and Halpain, S. (2000). Dynamic actin filaments are required for stable long-term potentiation (LTP) in area CA1 of the hippocampus. Proc. Natl. Acad. Sci. USA *97*, 6856–6861.

Lee, H.K., Takamiya, K., Han, J.S., Man, H., Kim, C.H., Rumbaugh, G., Yu, S., Ding, L., He, C., Petralia, R.S., et al. (2003). Phosphorylation of the AMPA receptor GluR1 subunit is required for synaptic plasticity and retention of spatial memory. Cell *112*, 631–643.

Lei, M., Lu, W., Meng, W., Parrini, M.C., Eck, M.J., Mayer, B.J., and Harrison, S.C. (2000). Structure of PAK1 in an autoinhibited conformation reveals a multistage activation switch. Cell *102*, 387–397.

Lisman, J.E. (2001). Three Ca2 levels affect plasticity differently: the LTP zone, the LTD zone and no man's land. J. Physiol. *532*, 285.

Lu, W., Man, H., Ju, W., Trimble, W.S., MacDonald, J.F., and Wang, Y.T. (2001). Activation of synaptic NMDA receptors induces membrane insertion of new AMPA receptors and LTP in cultured hippocampal neurons. Neuron *29*, 243–254.

Luo, L., Hensch, T.K., Ackerman, L., Barbel, S., Jan, L.Y., and Jan, Y.N. (1996). Differential effects of the Rac GTPase on Purkinje cell axons and dendritic trunks and spines. Nature *379*, 837–840.

Luscher, C., Nicoll, R.A., Malenka, R.C., and Muller, D. (2000). Synaptic plasticity and dynamic modulation of the postsynaptic membrane. Nat. Neurosci. *3*, 545–550.

Mackenzie, P.J., Kenner, G.S., Prange, O., Shayan, H., Umemiya, M., and Murphy, T.H. (1999). Ultrastructural correlates of quantal synaptic function at single CNS synapses. J. Neurosci. *19*, RC13.

Malenka, R.C., and Nicoll, R.A. (1993). NMDA-receptor-dependent synaptic plasticity: multiple forms and mechanisms. Trends Neurosci. *16*, 521–527.

Manser, E., Chong, C., Zhao, Z.S., Leung, T., Michael, G., Hall, C., and Lim, L. (1995). Molecular cloning of a new member of the p21-Cdc42/Rac-activated kinase (PAK) family. J. Biol. Chem. *270*, 25070–25078.

Markus, E.J., and Petit, T.L. (1987). Neocortical synaptogenesis, aging, and behavior: lifespan development in the motor-sensory system of the rat. Exp. Neurol. *96*, 262–278.

Martin, S.J., and Morris, R.G. (2002). New life in an old idea: the synaptic plasticity and memory hypothesis revisited. Hippocampus *12*, 609–636.

Matsuzaki, M., Ellis-Davies, G.C., Nemoto, T., Miyashita, Y., Iino, M., and Kasai, H. (2001). Dendritic spine geometry is critical for AMPA receptor expression in hippocampal CA1 pyramidal neurons. Nat. Neurosci. *4*, 1086–1092.

Matus, A. (2000). Actin-based plasticity in dendritic spines. Science *290*, 754–758.

Meng, Y., Zhang, Y., Tregoubov, V., Janus, C., Cruz, L., Jackson, M., Lu, W.Y., MacDonald, J.F., Wang, J.Y., Falls, D.L., and Jia, Z. (2002). Abnormal spine morphology and enhanced LTP in LIMK-1 knockout mice. Neuron *35*, 121–133.

Micheva, K.D., and Beaulieu, C. (1996). Quantitative aspects of synaptogenesis in the rat barrel field cortex with special reference to GABA circuitry. J. Comp. Neurol. *373*, 340–354.

Migaud, M., Charlesworth, P., Dempster, M., Webster, L.C., Watabe, A.M., Makhinson, M., He, Y., Ramsay, M.F., Morris, R.G., Morrison, J.H., et al. (1998). Enhanced long-term potentiation and impaired learning in mice with mutant postsynaptic density-95 protein. Nature *396*, 433–439.

Morales, M., and Fifkova, E. (1989). In situ localization of myosin and actin in dendritic spines with the immunogold technique. J. Comp. Neurol. *279*, 666–674.

Moser, M.B., Trommald, M., and Andersen, P. (1994). An increase in dendritic spine density on hippocampal CA1 pyramidal cells following spatial learning in adult rats suggests the formation of new synapses. Proc. Natl. Acad. Sci. USA *91*, 12673–12675.

Murthy, V.N., Schikorski, T., Stevens, C.F., and Zhu, Y. (2001). Inactivity produces increases in neurotransmitter release and synapse size. Neuron *32*, 673–682.

Myme, C.I., Sugino, K., Turrigiano, G.G., and Nelson, S.B. (2003). The NMDA-to-AMPA ratio at synapses onto layer 2/3 pyramidal neurons is conserved across prefrontal and visual cortices. J. Neurophysiol. *90*, 771–779.

Nakazawa, K., McHugh, T.J., Wilson, M.A., and Tonegawa, S. (2004). NMDA receptors, place cells and hippocampal spatial memory. Nat. Rev. Neurosci. *5*, 361–372.

Nusser, Z., Lujan, R., Laube, G., Roberts, J.D., Molnar, E., and Somogyi, P. (1998). Cell type and pathway dependence of synaptic AMPA receptor number and variability in the hippocampus. Neuron *21*, 545–559.

O'Donnell, W.T., and Warren, S.T. (2002). A decade of molecular studies of fragile X syndrome. Annu. Rev. Neurosci. *25*, 315–338.

Ostroff, L.E., Fiala, J.C., Allwardt, B., and Harris, K.M. (2002). Polyribosomes redistribute from dendritic shafts into spines with enlarged synapses during LTP in developing rat hippocampal slices. Neuron *35*, 535–545.

Parnas, D., Haghighi, A.P., Fetter, R.D., Kim, S.W., and Goodman, C.S. (2001). Regulation of postsynaptic structure and protein localization by the Rho-type guanine nucleotide exchange factor dPix. Neuron *32*, 415–424.

Paulsen, O., and Sejnowski, T.J. (2000). Natural patterns of activity and long-term synaptic plasticity. Curr. Opin. Neurobiol. *10*, 172–179.

Penzes, P., Beeser, A., Chernoff, J., Schiller, M.R., Eipper, B.A., Mains, R.E., and Huganir, R.L. (2003). Rapid induction of dendritic spine morphogenesis by trans-synaptic EphrinB-EphB receptor activation of the Rho-GEF kalirin. Neuron *37*, 263–274.

Ramon-Moliner, E. (1970). Contemporary Research Methods in Neuroanatomy (Berlin, Heidelberg, New York: Springer).

Regehr, W.G., and Stevens, C.F. (2001). Synapses (Baltimore: The Johns Hopkins University Press).

Renger, J.J., Egles, C., and Liu, G. (2001). A developmental switch in neurotransmitter flux enhances synaptic efficacy by affecting AMPA receptor activation. Neuron *29*, 469–484.

Sanders, L.C., Matsumura, F., Bokoch, G.M., and de Lanerolle, P. (1999). Inhibition of myosin light chain kinase by p21-activated kinase. Science *283*, 2083–2085.

Scheiffele, P. (2003). Cell-cell signaling during synapse formation in the CNS. Annu. Rev. Neurosci. *26*, 485–508.

Schikorski, T., and Stevens, C.F. (1997). Quantitative ultrastructural analysis of hippocampal excitatory synapses. J. Neurosci. *17*, 5858–5867.

Squire, L.R., and Alvarez, P. (1995). Retrograde amnesia and memory consolidation: a neurobiological perspective. Curr. Opin. Neurobiol. *5*, 169–177.

Takumi, Y., Ramirez-Leon, V., Laake, P., Rinvik, E., and Ottersen, O.P. (1999). Different modes of expression of AMPA and NMDA receptors in hippocampal synapses. Nat. Neurosci. *2*, 618–624.

Tonegawa, S., Nakazawa, K., and Wilson, M.A. (2003). Genetic neuroscience of mammalian learning and memory. Philos. Trans. R. Soc. Lond. B Biol. Sci. *358*, 787–795.

Toni, N., Buchs, P.A., Nikonenko, I., Bron, C.R., and Muller, D. (1999). LTP promotes formation of multiple spine synapses between a single axon terminal and a dendrite. Nature *402*, 421–425.

Toni, N., Buchs, P.A., Nikonenko, I., Povilaitite, P., Parisi, L., and Muller, D. (2001). Remodeling of synaptic membranes after induction of long-term potentiation. J. Neurosci. *21*, 6245–6251.

Trachtenberg, J.T., Trepel, C., and Stryker, M.P. (2000). Rapid extragranular plasticity in the absence of thalamocortical plasticity in the developing primary visual cortex. Science *287*, 2029–2032.

Trachtenberg, J.T., Chen, B.E., Knott, G.W., Feng, G., Sanes, J.R., Welker, E., and Svoboda, K. (2002). Long-term in vivo imaging of experience-dependent synaptic plasticity in adult cortex. Nature *420*, 788–794.

Tsien, J.Z., Huerta, P.T., and Tonegawa, S. (1996). The essential role of hippocampal CA1 NMDA receptor-dependent synaptic plasticity in spatial memory. Cell *87*, 1327–1338.

Turrigiano, G.G., and Nelson, S.B. (2000). Hebb and homeostasis in neuronal plasticity. Curr. Opin. Neurobiol. *10*, 358–364.

Vyas, A., Mitra, R., Shankaranarayana Rao, B.S., and Chattarji, S. (2002). Chronic stress induces contrasting patterns of dendritic remodeling in hippocampal and amygdaloid neurons. J. Neurosci. *22*, 6810–6818.

Willshaw, D.J., and Dayan, P. (1990). Optimal plasticity from matrix memories: what goes up must come down. Neural Comput. *2*, 85–93.

Yuste, R., and Bonhoeffer, T. (2001). Morphological changes in dendritic spines associated with long-term synaptic plasticity. Annu. Rev. Neurosci. *24*, 1071–1089.

Zenke, F.T., King, C.C., Bohl, B.P., and Bokoch, G.M. (1999). Identification of a central phosphorylation site in p21-activated kinase regulating autoinhibition and kinase activity. J. Biol. Chem. *274*, 32565–32573.

Zeng, H., Chattarji, S., Barbarosie, M., Rondi-Reig, L., Philpot, B.D., Miyakawa, T., Bear, M.F., and Tonegawa, S. (2001). Forebrain-specific calcineurin knockout selectively impairs bidirectional synaptic plasticity and working/episodic-like memory. Cell *107*, 617–629.

Zhao, Z.S., Manser, E., Chen, X.Q., Chong, C., Leung, T., and Lim, L. (1998). A conserved negative regulatory region in alphaPAK: inhibition of PAK kinases reveals their morphological roles downstream of Cdc42 and Rac1. Mol. Cell. Biol. *18*, 2153–2163.

Zucker, R.S. (1989). Short-term synaptic plasticity. Annu. Rev. Neurosci. *12*, 13–31.